UNIVERSIDAD CATÓLICA DE TEMUCO

MAGÍSTER EN RECURSOS NATURALES
FACULTAD DE RECURSOS NATURALES

TESIS

ORIGIN OF HOTSPRINGS NEAR VILLARRICA VOLCANO

Presentada como parte de los requisitos para optar al grado de Magíster en Recursos Naturales

Por

Claudia Bucarey Parra

TEMUCO – CHILE

2019

Trabajo de Grado: Origin of hotsprings near Villarrica volcano.
Estudiante: Claudia Andrea Bucarey Parra
Magíster en Recursos Naturales

COMISIÓN DE GRADO

Ministro de Fe: ……
Pamela Sánchez Pérez
Magíster en Ciencias, mención Ecología
Universidad Católica de Temuco

Profesor Guía: ……
Francisco Encina Montoya
Doctor en Ciencias Ambientales
Universidad Católica de Temuco

Profesor Informante: ……
Elisa Ramírez Sánchez
Doctora en Ciencias, mención Geología
Universidad Católica de Temuco

Profesor Informante: ……
Gabriela Velásquez Vargas
Doctora en Ciencias de Recursos Naturales
Servicio Nacional de Geología y Minería

TEMUCO, junio 2019

ÍNDICE DE CONTENIDOS **Página**

RESUMEN

El volcán Villarrica es uno de los volcanes más activos de la Zona Volcánica de Los Andes del Sur (SAVZ) y presenta varias manifestaciones termales en sus alrededores. Si bien existen numerosos estudios acerca de la composición y origen de las aguas termales de esta zona, no se ha podido establecer cuál es la influencia de la actividad volcánica en estas manifestaciones. La mayoría de las termas ubicadas cerca de la zona volcánica, entre las ciudades de Pucón y Curarrehue, fueron muestreadas entre los años 2012 y 2017. En este estudio, identificamos los procesos que afectan la composición de las aguas y que puedan explicar el origen y su naturaleza. Análisis químicos fueron realizados permanentemente, con el objetivo de describir la composición química de las aguas termales, y con esta información entender el comportamiento de las aguas en profundidad. Así mismo, se implementó por primera vez en esta zona de estudio, el análisis de gas disuelto en agua. Estas manifestaciones emergen directamente desde granitoides, depósitos volcanoclásticos, piroclásticos y fluviales. Los parámetros fisicoquímicos tales como: temperatura, pH y sólidos disueltos totales (TDS) fueron medidos in-situ. Nuestros resultados muestran que las temperaturas en un rango entre 29 y 87ºC son comunes en estas aguas mesotermales y los valores de pH permiten clasificar estos fluidos como neutros – alcalinos (pH=7.0 – 9.7). Las manifestaciones presentan concentraciones de iones en rangos bajos y moderados (TDS=76 – 656 mg/L). Las aguas y los gases disueltos fueron muestreados para analizar elementos mayores, trazas e isótopos (^{18}O-D). Con estos datos, se observó una mezcla de procesos en los cuales las recargas meteóricas del sistema y su interacción en profundidad con gases magmáticos, son los principales mecanismos de generación de la termalidad de esta zona.

Palabras clave: Geoquímica, Aguas Termales, Gas Disuelto.

ABSTRACT

The Villarrica volcano is one of the most active volcanoes of the Southern Andes Volcanic Zone (SAVZ) and has several thermal manifestations in their surroundings. Although there are numerous studies about the composition and origin of the thermal waters of this area, it has not been possible to establish which is the influence of volcanic activity in these manifestations. Most hotsprings located close to the Villarrica volcano, between Pucón and Curarrehue locations were sampled during 2012 and 2016. In this study, we identify the processes that affect the composition of the water that can explain the origin and its nature.Chemical analyzes were carried out permanently, with the objective of describing the chemical composition of the thermal waters, and with this information to understand the behavior of the waters in depth. Likewise, the analysis of gases dissolved in water was implemented for the first time in this area of study. This manifestation emerges directly from granitoides, volcanoclastic, pyroclastic and fluvial deposits. Physicochemical parameters such as: temperature, pH, and total dissolved solids (TDS) were measured in-situ. Our results showed that temperatures ranging between 29 – 87 °C, are common in these mesothermal waters, and pH allows to classify these fluids as neutral to alkaline waters (pH=7.0 to 9.7). Hot springs present low to moderate concentrations of ions (TDS= 76 to 656 mg/L). Water and dissolved gases were sampled to analyze main elements, traces and isotopes (^{18}O – D). With these data, a mixture of processes was observed in which the meteoric recharges of the system and their deep interaction with magmatic gases are the main mechanisms of generation of the thermal manifestations of this zone.

Key words: Geochemistry, Thermal waters, Dissolved Gases.

INTRODUCTION

In Southern Chile, the hydrothermal activity is due to a combination of high geothermal gradients as a consequence of recent magmatic activity, the presence of permeable host rocks and an abundant meteoric recharge, like snowmelts, rainfalls and surface runoffs of rivers (Ray et al., 2009).

Several processes has been described with the aim to understand the origin of dissolved components in the Chilean thermal waters, where salts contributions have major impacts on the composition of subsurface waters in northern Chile (Risacher et al., 2011), whereas in southern Chile thermal waters are intended as two main processes: 1. mixing with sea water (Perez, 1999; Risacher et al., 2011) and 2. deep magmatic contribution (Sepúlveda et al., 2007; Ray et al., 2009; Benavente et al., 2015;Tardani et al, 2016; Roulleau et al., 2017).

The main thermal manifestations located between latitudes 38°-39°S has been characterized by many authors (Hauser, 1989, 1997; Pérez, 1999; Sepúlveda et al., 2007; Risacher & Hauser, 2008; Risacher et al, 2011) being thus a wide database available. However, it is still unclear the dominant processes that give rise to thermal waters, and therefore the volcanic-tectonic environment can probably fall into ambiguities (Alam et al., 2013).

In this work, we study chemical and isotopic data from thermal waters and gases dissolved in water for the first time. This last technique, will allow us to know the composition of the gases in the thermal manifestations, which will give us lights about the magmatic contribution in each study area.

GEOLOGICAL AND VOLCANOLOGICAL SETTINGS

The characteristics of the convergence of the Nazca and the South American Plates exert a control to all the volcanic and seismic activity in the Southern Andes. Thus, geometrics variations in Wadati-Benioff zone generates a division in the quaternary Andean volcanic arc in 3 segments, denominated as Central Volcanic Zone (CVZ: 17°- 28°S), Southern Volcanic Zone (SVZ: 33°- 46°S) and Austral (far southern) Volcanic Zone (AVZ: 48°-56°S) (Lopez-Escobar et al., 1995) (Fig. 1). SVZ magmetism is mostly controlled by the dehydration of the Nazca plate and/or the melting of the subducted oceanic lithosphere, resulting in the addition of subducted components, and the melting of the overlying mantle wedge (Thorpe, 1984; Stern, 2004). The crust below the SVZ consists of Palaeozoic and Mesozoic pre-Andean basement and Mesozoic-Cenozoic igneous rocks and has a

close relation with the Liquiñe-Ofqui fault zone (LOFZ), a major intra-arc fault system that dominates this region. Ductile-to-brittle shear zones documents that the LOFZ have been active as a transpressional dextral strike-slip structure at least over the last 6 Ma (Cembrano et al., 2009), although geologic evidence suggest the LOFZ was probably a leaky transform fault for about 25 Ma (Herve et al., 1993). This fault system controls the location of many of the larger volcanic centers, as well as smaller eruptive centers of the monogenetic cones in the southern SVZ (Lopez-Escobar et al., 1995) so therefore acquires importance to be recognized as a principal way for the vertical migration of fluids (Sibson 1994, 1996; Rowland and Sibson, 2004; Rowland and Simmons, 2012; Tardani, 2016).Post-glacial eruptions of SVZ volcanoes include the full range of Hawaiian, Strombolian, Subplinian, Plinian, Vulcanian and Phreatomagmatic types, with a VEI (Newhall & Self 1982) ranging from 0 to 6. There seems to be a relationship between magma composition and the eruption style. Basaltic to basaltic - andesitic magmas have mainly Strombolian eruptions, which normally can also include Hawaiian phases, such as the typical historic eruptions of the Llaima and Villarrica volcanoes, the most active in Chile.

Villarrica is a Middle Pleistocene to Holocene compound volcano (Moreno and Clavero, 2006) extremely active and mainly basaltic to andesitic stratovolcano, with more than 49 eruptions since 1558 (Petit-Breuilh, 1994; Lara, 2004a). It is located on the western edge of the Villarrica – Quetrupillán – Lanín volcanic chain (López-Escobar et al., 1995; Stern et al., 2007) aligned parallel to the Gastre Fault Zone (Bohm et al., 2002) (Fig. 1), affecting the basement rocks. South of the volcanic chain, prevails the plutonic rocks of the North Patagonian Batholit (Hervé, 1984; Munizaga et al., 1988), consisting of plutonic rocks from dioritic to tonalitic composition (Adriasola et al., 2005); while in the north, the plutonic basements overlaying by the volcano-sedimentary Cura-Mallín formation (Jordan et al., 2001), which is associated as a host of the geothermal reservoirs in Southern Chile (Sanchez-Alfaro et al., 2016).

Villarrica is 2847 m.a.s.l. high and its activity started at least 600 ky ago (Moreno and Clavero, 2006), producing basalts and basaltic andesite lava flows as well pyroclastic deposits. The Villarrica volcano edifice is constructed of pyroclastic flows and scoria fall deposits as well as ‘aa’ a pahoehoe lavas (Witter et al., 2004). This volcano has shown recurrent postglacial explosive activity, similar to other volcanoes of the Southern Andes (37°-42°S) (Stern, 2004), interspersed with and usual effusive activity (Moreno, 1974; Lopez-Escobar, 1995), being one of the three most active volcanoes in South America (Witter et al., 2004). Postglacial eruptive activity formed volcanic boilers which are

associated with 10 km3 basaltic andesite Licán Ignimbrite and the 5 km3 basaltic andesite Pucón Ignimbrite (Clavero and Moreno, 1994; Moreno et al., 1994a). Since the large eruption in 1984-1985, the summit of the Villarrica has been occupied by a persistently degassing lava lake, frequently perturbed by strombolian eruptions and fountaining (Calder et al., 2004). Activity of Villarrica has been characterized by frequent small as well highly explosive eruptions, being the last paroxysmal eruption in March 2015, punctuated by VEI ≈ 2 explosive events and lahars (Aiuppa et al., 2017). Currently this activity is characterized by an actively degassing lava lake level, inside the crater and thermal activity.

Several hotsprings can be observed in the surroundings of the Villarrica volcano (Fig. 2), which represents touristic advantages, mainly during the winter season. Despite thermal manifestations has been characterized, still it is unclear the dominant processes that governs them, and therefore which is the role of volcano-tectonic environment in the origin of these thermal manifestations. The goal of this study was to characterize the main thermal waters and a group of them, according to the dominant chemical composition and recognize some main processes that govern the origin of these hotsprings.

MATERIALS AND METHODS

Water and dissolved gas sampling

All the hydrothermal discharges consists of hotsprings where there are no indications about fumaroles near to the volcanoes (Witter et al., 2004). In the present study, 16 thermal water samples from different sites and 2 cold water samples from Palguín and Aitué rivers were collected between 2012 and 2017 in the Araucania Region. Temperature, pH and conductivity were measured in situ with portable instruments (uncertainty: ± 0.1 °C, ± 0.01 and 2% respectively). Samples for cations and trace elements were collected in 125 mL bottles, filtered through a 0.45 µm filter acidified with concentrated HNO_3 1 mL in 100 mL sample. Water samples for anions analyses were collected unfiltered in 125 mL bottles. Additionally, 50 mL of diluted water samples (1:10) in situ were collected for SiO_2 analysis. The $\delta D\text{-}H_2O$ and $\delta^{18}O\text{-}H_2O$ samples were collected in 100 mL dark glass bottles. Besides, 9 water samples for dissolved gases determination were collected using pre-evacuated 250 mL Pyrex flasks equipped with Thorion®. The glass bottles were filled with about ¾ of their inner volume according to Tassi et al. (2009) and Capecchiacci et al.(2015).

Chemical and isotopic analyses of waters

Major cations like Na^+, K^+, Ca^{2+}, Mg^{2+} and Li^+ were determined by atomic absorption spectrophotometry (AAS) (Perkin Elmer PE4000), NH_4^+ by ion-selective electrode method (ISE)(EA-920) and anions (Cl^-, SO_4^{2-}, F^- and NO_3^-) were analyzed by ion-chromatography (IC) (Dionex ICS-3000). The concentration of HCO_3^-/CO_3^{2-} was calculated by acidimetric titration with H_2SO_4. SiO_2, B, Sr^{2+} and trace elements (i.e. Al, Sb, As, Ba, Be, Cd, Ce, Co, Cu, Cr, Sn, P, Fe_{tot}, Mn, Mo, Ag, Pb, Rb, Se, Va, and Zn) were analyzed using inductively coupled plasma mass spectrometry (ICP-MS) (Agilent 7500a) at the SERNAGEOMIN Chemical Laboratory.

The $^{18}O/^{16}O$ and $^{2}H/^{1}H$ isotopic ratios, expressed as $\delta D\text{-}H_2O$ and $\delta^{18}O\text{-}H_2O$ ‰ V-SMOW, were determined by mass spectrometry (Finnigan MAT 252 and Europa Scientific GEO2020 respectively). Oxygen isotopic ratios were analyzed on CO_2 added to the water samples using de CO_2-H_2O equilibration method proposed by Epstein and Mayeda (1953). Hydrogen isotopic ratios were measured on H_2 generated by the reaction of 10 µL of water with metallic zinc at 500°C (Coleman et al., 1982). The analytical uncertainties for $\delta D\text{-}H_2O$ and $\delta^{18}O\text{-}H_2O$ ratios were 0.1‰ and 1‰, respectively.

Chemical analyses of dissolved gases

The composition of the main inorganic compounds (CO_2, N_2, Ar, O_2, Ne y He), stored in the flasks headspace were analyzed using a gas chromatograph (GC) equipped with a 9 m long 5A molecular sieve column and a thermal conductivity detector (TCD) (Shimadzu 15 A). The CH_4 analysis was carried out using a Shimadzu 14A gas chromatograph equipped with a Flame Ionization Detector (FID) and a 10 m long stainless steel column packed with Chromosorb PAW 80/100 mesh coated with 23% SP1700 (Vaselli et al., 2006; Tassi et al., 2009; Capecchiacci et al., 2015). The analytical error for GC analysis was ≤5%.

RESULTS

Physicochemical parameters and major ion chemistry

Table 1 shows the concentrations of the major and trace elements measured as well as the physicochemical parameters of the thermal waters sampled in this study. Thermal waters discharges have outlet temperatures between 30° and 71°C, the pH ranged between 7.1 and 9.3, and total dissolved solids (TDS) between 109 and 575 mg/L. The samples were divided into three groups based on major anion concentrations: (i) sulfate waters (SO_4^{2-}), (ii) bicarbonate waters (HCO_3^-), and (iii) sulfate-bicarbonate (SO_4^{2-}-HCO_3^-) waters. 11 out of 18 samples can be classified as sulfate waters, 3 as HCO_3 waters and 4 as SO_4^{2-}-HCO_3^- waters, using the classification diagram of Langelier & Ludwig (1942)(Fig. 3).

The sulfate group had a sodium like as the dominant cation and temperatures and pH values ranged from 33° to 66°C and 7.2 to 9.3 respectively, containing different levels of SO42− (65–342 mg/L) and similar amounts of Na (52 – 73 mg/L) except in GEO and COF, where the concentrations were 137 and 160 mg/L respectively, containing a low Cl-concentration s (7.4 - 51 mg/L) and low HCO3- values (35 - 69 mg/L). Main cations (Ca2+, K+ and Li+) concentrations ranged between 5.8 - 47 mg/L, 0.9 - 5.4 mg/L and 0.02 – 0.2 mg/L respectively (Table 1).

The second group (HCO_3^-) had a sodium-calcium like as the dominant cations. In this case, two samples corresponding to cold waters (AIT and RPA) showed low temperatures (4° – 7°C) and almost a neutral pH (7.3 and 7.5 respectively). Their chemical concentrations were very low, consistent with the typical cold spring values (Table 1). The third sample was Na-HCO_3 type, with temperature and pH values of 43 °C and 7.1 respectively. Low Na^+ values were detected (29 mg/L), like in similar cases of others main ions (4.4 mg/L for Cl^-; 30 mg/L for SO_4^{2-}; 7.0 mg/L for Ca^{2+}; 1.7 mg/L for K^+ and 0.02 for Li^+).

As in the previous group, the third classification had Na^+ like as the dominant cation. Their temperatures and pH values ranged from 42° to 71°C and 7.8 and 8.7 respectively, containing similar HCO_3^-/SO_4^{2-} ratios (1.2 - 1.3) except in PAL, where the ratio between both anions were 3.1.

These samples showed different amounts for the main ions, covering a range between 33 – 100 m/L for SO_4^{2-}, 72-123 mg/L for $HCO_3^-$and 12 - 84 mg/L for Cl^-. Main cations (Ca^{2+}, K^+ and Li^+) concentrations ranged between 2.0 – 5.0 mg/L, 2.2 - 4.8 mg/L and 0.02 – 0.14mg/L respectively.

Regarding to the trace elements concentrations (Table 2), the highest B values were measured at GEO and COF (3.2 and 2.4 mg/L respectively) ranging between 0.1 – 3.2 mg/L, followed by As (from 0.005 to 1.18 mg/L). No significant values of trace elements were measured. The ^{18}O-H_2O and D-H_2O values (Table 1) of the $Na^+SO_4^{2-}$ waters ranged from -6.7 to -9.6 and -78 to -61 ‰ vs. V-SMOW, respectively. For $Na^+HCO_3^-$ waters, values ranged from -7.5 to -9.1 and -74 to -56 ‰ vs. V-SMOW, respectively. The ^{18}O-H_2O and D-H_2O values of the cold waters samples ranged from -7.5 to -7.9 and -58 to -57 ‰ vs. V-SMOW.

Chemical compositions of the dissolved gases

The chemical composition (in mmol/mol) of the dissolved gases are shown in Table 3, where the ^{13}C-CO_2 (in ‰ vs. V-PDB) values are also reported. Nitrogen was largely the most abundant gas species (from 585 to 814 mmol/mol), followed by CO_2 (from 74 to 378 mmol/mol), O_2 (from 13 to 194 mmol/mol), Ar (from 15 to 20 mmol/mol), CH_4 (from 0.013 to 0.081 mmol/mol), He (from 0.015 to 0.030 mmol/mol) and Ne (from 0.0073 to 0.010 mmol/mol). The ^{13}C-CO_2values ranged from -13.9 to -25.2 ‰ vs. V-PDB.

DISCUSSION

Gas discharges

The relative distribution of N_2, He and Ar are plotted on the triangular diagram and used as a source indicator of the origin of volatile components of Fig. 4 (after Giggenbach and Goguel, 1989; Giggenbach and Poreda, 1993). Gas compositions from the Villarrica area were consistent with the ASW (Air Saturated Water), suggesting a dominant atmospheric origin for the three species, consistent with those data previously published by Ray et al. (2009).

Nevertheless, the diagram Ar-O_2/10-1000*Ne, shows a strong decrease in the relative concentrations of O_2, suggesting a consumption during water-rock interactions, product of the occurrence of the redox reactions between the different gaseous species. The O_2 consumption is considerably strong in almost all hot springs, except in the Pellaifa and Culan waters, probably due to a greater recharge with the groundwater system (Fig. 5).

All the samples had dissolved CO_2 contents higher than those in equilibrium with the atmosphere (ASW), thus suggesting a direct input of CO_2- rich fluids and is probably likely related to three possible sources: i) dissolution of carbonate rocks, ii) oxidation of organic matter and iii) mantle or crustal degassing (Capecchiacci et al., 2015). It is reasonable to think in oxygen consumption due the reduced redox conditions, as a process causing the relative N_2-enrichment (Grassa et al., 2006). Almost all waters analyzed in this study are connected to active volcanic areas so their dissolved CO_2 contents are the consequence of intense interaction processes between groundwater and deep volcanic fluids emitted from anomalous soil CO_2-degassing zones (Anza et al., 1989; Allard et al., 1997; Badalamenti et al., 1988; D'Alessandro and Parello, 1997; Favara et al., 2001a). Considering the relatively low contents of CO_2 compared to other studies, it is probably that hot springs locations in volcanic areas can have low CO_2fluxes.

Although the carbon dioxide is an extremely reactive gas having high solubility in water (up to 760 ml per liter of pure water at STP conditions), physic-chemical conditions of groundwater can also affect the dissolution process of CO_2 into the thermal aquifers, being the relative abundance of the dissolved inorganic carbon species (CO_2 (aq), HCO_3^- and CO_3^{2-}) strongly dependent on the pH values of the waters. For these reasons, in thermal water with alkaline pH, the CO_2 dissolutions processes can be masked due to the conversion of carbon dioxide into dissolved bicarbonate (HCO_3^-) and carbonate (CO_3^{2-}) ions (Grassa et al., 2006). In other hand, considering the existence of LOFZ; deep tectonic discontinuities seem to play an important role in controlling the rising of both, thermal waters and deep gases towards the surface, acting as zones of high permeability

Thermal water discharges

Surface discharges from Villarrica thermal waters are dominated by alkaline sulphate-type springs. The chemistry of these springs and the prominent degassing from the lava lake of the Villarrica volcano (Witter et al., 2004) validates that absorption and condensation of the gaseous phase rich in sulphur species and low in chloride, this causes the $NaSO_4$ type waters, consistent with the values of chemical compounds and gas dissolved data.

Bicarbonate waters are most likely formed through the direct absorption of CO_2 from magmatic steam as it is condensed into the cool groundwater at the peripheries of volcanic systems (Ellis and Mahon, 1977; Giggenbach 1993; Simmons and Browne, 2000; Arnórsson et al., 2007).

The ternary diagram proposed by Giggenbach (1988) (Fig. 6) is widely used and based on the concentrations of the major chlorine (Cl^-), sulfate (SO_4^{2-}) and bicarbonate (HCO_3^-) anions. Although the classification is based on the chemical composition of water, this diagram makes possible to relate the relative content of anions to the origin of the fluids and/or processes occurring in their ascent to the surface. In this way, the neutral chlorinated waters suggest to represent the well-balanced fluids of the *upflow* zones, since the rapid rise of the geothermal waters allows the retaining of the original chemical composition (Giggenbach, 1988). The mixture of these waters with bicarbonate-rich groundwater, as is normally the case of meteoric waters, converts them into bicarbonate waters with a low concentration of Cl related to Na-Cl waters, generating a displacement towards the field of the peripheral waters. The absorption and condensation of steams and gases by groundwater, suspended aquifers, meteoric water of shallow infiltration, or volcanic lakes, generates "steam-heated" thermal waters. The mixture with H_2S of volcanic origin generates a displacement towards the sulphated water field due to the formation of HSO_4- ions, and due to the oxidation of H_2S. (Chandrasekharam and Bundschuh, 2008). If vapors are rich in CO_2, relatively acidic sulphated-bicarbonated waters can thus be obtained. However, exceptionally neutral – slightly alkaline sulphated - bicarbonated compositions can be obtained, indicating a possible neutralization of these waters by contact in the subsurface with the box rock (Sepulveda, 2005).

The stable isotopes are extremely useful tracers with respect the origin of geothermal fluids and secondary processes that have affected them, such as boiling, mixing and evaporation. The isotope of oxygen, ^{18}O and hydrogen, ^{2}H or D (deuterium), are the most used in geothermal exploration. The concentration of these isotopes can be obtained by comparing the mass ratios $^{18}O/^{16}O$ and D/H with respect to the standard V-SMOW (Vienna-Standard Mean Oceanic Water) in per thousand (‰). From another perspective, Giggenbach (1992) with more isotope data from thermal waters and fumarolic condensates of andesitic volcanoes, points to the existence of a positive shifting, not only in the values of $\delta^{18}O$ but also in δD, with regarding local meteoric waters. Based on the observation, the shift of δD pointed mainly towards the composition of condensates from volcanic fumaroles, Giggenbach (1992) postulates the existence of a member of fixed composition, called "andesitic water", which participates variably in mixing processes with both geothermal and volcanic discharges. One of the localities that do not verify this hypothesis corresponds to El Tatio Geyser, in northern Chile, where the deuterium shift is negative (Sepúlveda, 2005). This could be a complementary explanation of positive shifting in geothermal waters.

Considering these backgrounds we consider that the thermal waters that have meteoric origins will conserve its isotopic content. On the opposite, those fluids that are subjected to isotopic exchange at high temperatures and for sufficient time, or that they are the result of mixing with "andesitic waters", will reveal their origin through a positive shifting with respect to the local meteoric waters (Fig. 7).

Geothermometry

One of the geothermometers used in this study wasbased on the dissolution of silica,

$$SiO_2 + 2H_2O \rightarrow H_4SiO_4$$

(Eq.1)

where it is assumed that both water and silica are pure compounds, so the equilibrium constant becomes equal to a_{H4SiO4}. In addition, the activity coefficient of neutral species such as H_4SiO_4 is close to 1, so the equilibrium constant for the reaction (Eq. 1) is equal to the concentration of H_4SiO_4. By inserting these results into the equation, the balance of silica is modeled according to the following relationship:

$$\ln m_{H_4SiO_4} = \frac{a}{T} + b$$

(Eq. 2)

Using the silica concentration, C_{SiO2}, the expression is as follows:

$$\ln C_{SiO_2} - \ln MW_{SiO_2} = \frac{a}{T} + b$$

(Eq. 3)

Where MW_{SiO2} is the molar weight of silica.

At temperatures below 340°C, the solubility of all silicate minerals is proportional to the temperature (Fourier, 1991). In the case of silica, the dependence of the solubility of its polymorphs with temperature can be observed in Fig. 8, where in a range between 20º and 250ºC, behaves as straight

line (Fournier, 1973). At temperatures below 300 °C, variations in pressure at hydrostatic conditions have little preponderance in the solubility of amorphous silica and quartz (Fournier and Potter, 1982a, Fournier and Rowe, 1977) and the addition of dissolved salts has a significant effect only at concentrations greater than 2-3 wt% (Fournier, 1985, Fournier and Marshall, 1983). At temperatures above 300 °C, small variations in salt or pressure concentrations are very important in solubility as well as pH variations, for pH greater than 7.5, due to the silica speciation. Fig. 8 shows that according the mineral phase that controls the solubility of silica, there will be different fluid-mineral balance curves. Using silica concentration, C_{SiO2}, the equation is as follows, as proposed by Fournier:

Quartz without loss of steam (50 – 250ºC)

$$T\ (°C) = \frac{1309}{(5{,}19 - \log C_{SiO2}} - \ 273{,}15$$

(Eq. 4)

Quartz with maximum steam loss (100 – 250 ºC)

$$T\ (°C) = \frac{1522}{(5{,}75 - \log C_{SiO2}} - \ 273{,}15$$

(Eq. 5)

Chalcedony (50 – 250 ºC)

$$T\ (°C) = \frac{1032}{(4{,}69 - \log C_{SiO2}} - \ 273{,}15$$

(Eq. 6)

α-cristobalite (100 – 250 ºC)

$$T\ (°C) = \frac{1000}{(4{,}78 - \log C_{SiO2}} - 273{,}15$$

(Eq. 7)

Amorphous silica

$$T\ (°C) = \frac{731}{(4{,}52 - \log C_{SiO2}} - 273{,}15$$

(Eq. 8)

Applying silica geothermometers with temperature values recorded on field samples of thermal manifestations in this study, the equilibrium temperature values can be obtained with those silica phases (Table 4). There is an ambiguity in the selection of the correct geothermometer since the mineral phase that controls the solubility of the silica must be determined. At temperatures higher than 180ºC, quartz is the main phase that controls the solubility of silica (Fournier, 1991). While at temperatures between 120 - 180°C, chalcedony appears together with quartz. The precipitation of one of these two phases depends exclusively on the growth of the crystals, since chalcedony is a cryptocrystalline variety of quartz, so variables such as temperature, residence time and fluid composition will control the appearance of one of the two phases at the temperatures mentioned before (Fournier, 1991).

Finally, at temperatures below 120 °C, cristobalite is the most commonly considered phase. In some cases, the solubility of the silica can be determined by the amorphous silica. Fournier (1985) noted that the reaction kinetics of amorphous silica is relatively faster than that of quartz and chalcedony, so in hot springs in equilibrium with sinter silica (fine-grained precipitations composed essentially of amorphous silica) will rarely be preserved concentrations greater than 350 ppm of SiO_2, which will impose maximum temperatures for these geothermometers.

The results obtained by applying different silica geothermometers are shown in Table 4. The temperatures obtained through the geothermometers based on silica concentrations may be very reliable and appropriate considering the variations of silicia speciation with pH and temperature. In all this cases the temperature is less than in the upwelling zone. because SiO_2 has a volatile behavior

only at temperatures higher than 350ºC, an event of steam loss at lower temperatures will cause an increase in the concentration of this in the fluid, determining higher equilibrium temperatures than the true ones. On the opposite, processes such as the dilution of thermal waters with meteoric waters, will cause a decrease in the concentration of silica, which will lead to an underestimation of the temperature equilibrium.

Geothermometers based on cationic ratios such as Na-K (Fournier, 1979) and K-Mg (Giggenbach, 1988) provides powerful tools for assessing conditions in the depths of geothermal systems (Giggenbach and Gouguel, 1989). This because they are less to modify by secondary effects processes such as dilution or boiling, respect to those based on individual components. The main problems associated to its use, comes from the use of samples that are inadequate. To increase the reliability of results, Giggenbach (1988) proposed to combine a medium triangular diagram to fast K-Mg geothermometer response, with the Na-K geothermometer of slow rebalancing, and thus obtain a method to evaluate the degree of balance water rock that has reached a geothermal fluidity. This uses the temperature dependence of two reactions where feldspars and others minerals are involved. Based on feldspars, there are two geothermometers, one of them proposed by Forunier (1979) from the empirical data:

$$T\ (°C)\ =\ \frac{1217}{\log\frac{Na}{K} -\ 1{,}483} -\ 273$$

(Eq.1)

and the other proposed by Giggenbach (1988) from experimental data:

$$T\ (°C)\ =\ \frac{1390}{\log\frac{Na}{K} -\ 1{,}75} -\ 273$$

(Eq. 2)

The same author, proposed for the Eq.2:

$$T\ (°C)\ =\ \frac{1390}{14 + \log\frac{K^2}{Mg}} -\ 273$$

(Eq.3)

This way, the Na-K-$Mg^{1/2}$ diagram allows the iso-ratios Na/K and K/$Mg^{1/2}$ to be represented with straight lines, joining the apex of Mg and Na, with the opposite segment, respectively. Since each Na/K and K/$Mg^{1/2}$ ratio is equivalent to a single temperature in the geothermometers, these lines are isotherms (Fig. 8). Thus, the intersections of Na-K and K-Mg isotherms, corresponding to the same temperature, are chemical compositions of the fluid that is in equilibrium with the mineral phases that control both geothermometers, delineating the curve call of total equilibrium (Giggenbach, 1988). For those located in the field of "immature waters" the application of geothermometers of K-Na and K-Mg becomes dubious and we should be very careful in the interpretation of the suggested temperatures. The field at the lower end shows the compositional range that would present a generated fluid that conserves composition of the rock, in the limit case of dissolution.

Our results obtained in the volcanic area of Villarrica, are far from the typical characteristics of thermal zones in volcanic environments (Giggenbach & Goguel, 1989; Sepúlveda *et al*., 2004). It is highly probable to find extremely acidic manifestations (pH <2), with high contents of dissolved solids and temperatures that can easily exceed 80°C. However, despite the fact that the study area is contained in an active volcanic zone, they do not present the typical characteristics of volcanic waters. According to the results of the chemical and gas analyzes, there is a strong interaction with meteoric waters and a clear dilution with components similar to those of river waters adjoining the thermal manifestations. Despite being to a proximal volcanic zone, apparently the magmatic influence is not enough to add the signature of volcanic waters to these springs.

CONCLUSIONS

The chemical and isotopic compositions of waters and gases of the Villarrica volcano show a mixture of processes that give rise to their nature. A large meteoric recharge caused by the climate of the area and the addition of magmatic gases in low proportions shown in the chemistry of dissolved gases, gives rise to this type of sulfated-bicarbonate manifestations. This is supported by the low values of TDS and pH values far from the typical sulphated acidic waters, which agrees with a magmatic contribution and subsequent neutralization due to the interaction of water rock and mixture of these fluids with surface water. The isotopes of ^{18}O and D, indicate that the origin of the fluids associated with the thermal waters comes from the percolation and subsequent heating of meteoric

waters, which then ascend by density difference. The geothermometry showed that only 4 (GEO, COF, PFA and CON) out of 16 thermal water samples were possible to evaluate, reaffirming that most of thermal manifestations are related with meteoric recharge and groundwater, heated during they circulation.

REFERENCES

Adriasola, A.C., Thomson, S.N., Brix, M.R., Hervé, F,, Stöckhert, B.,2005. Postmagmatic cooling and late Cenozoic denudation of the North Patagonian Batholith in the Los Lagos region of Chile, 41°-42°15'S. International Journal of Earth Science, 95, 504-528.

Aiuppa, A., Bitetto, M., Francofonte. V., Velasquez, G., Bucarey-Parra, C., Giudice, G., Liuzzo, M., Moretti, R., Moussallam, Y., Peters, N., Tamburello, G., Valderrama, O.A., Curtis, A., 2017. A CO2-gas precursor to the March 2015 Villarrica volcano eruption. Geochemistry, Geophysics, Geosystems, 18(6), 2120-2132.

Alam, M.A., Parada, M.A.,2013. A note on "Origin of components in Chilean thermal waters" by Risacher et al. (2011). Journal of South American Earth Sciences, 69, 259-261.

Allard, P., Jean-Baptiste, P., D'Alessandro, W., Parello, F., Parisi, B., Flehoc, C., 1997. Mantle-derived helium and carbon in groundwaters and gases of Mount Etna, Italy. Earth Planet Science Letters, 148, 501-516.

Anzà, S., Dongarrà, G., Giammanco, S., Gottini, V., Hauser, S., Valenza, M., 1989. Geochimica dei fluidi dell'Etna: Le acque sotterranee. Mineralogy and Petrography Acta, 32, 231-251.

Arnórsson, S., Stefánsson, A., Bjarnason, J.Ö., 2007 Fluid-fluid interaction in geothermal systems. Reviews in Mineralogy and Geochemistry, 65, 259-312.

Badalamenti, B., Gurrieri, S., Hauser, S., Parello, F., Valenza, M., 1988. Soil CO2 output in the island of Vulcano during the period 1984--1988: Surveillance of gas hazard and volcanic activity. Rendiconti della Societa Italiana di Mineralogia e Petrologia, 43, 893-899.

Benavente, O., Tassi, F., Reich, M., Aguilera, F., Capecchiacci, F., Gutierrez, F., Vaselli, O., Rizzo, A., 2016. Chemical and isotopic features of cold and thermal fluids discharged in the Southern Volcanic Zone between 32.5°S and 36°S: Insights into the physical and chemical processes controlling fluid geochemistry in geothermal systems of Central Chile. Chemical Geology**,** 420, 97–113.

Bohm, M., Lüth, S., Echtler, H., Asch, G., Bataille, K., Bruhn, C., Rietbrock, A., Wigger, P., 2002. The Southern Andes between 36° and 40° latitude: seismicity and average seismic velocities. Tectonophysics, 356, 275-289.

Calder, E., Harris, A., Peña, P., Pilger, E., Flynn, L., Fuentealba, G., Moreno, H., 2004. Combined thermal and seismic analysis of the Villarrica volcano lava lake, Chile. Revista Geológica de Chile, 31, 259-272.

Capecchiacci, F., Tassi, F., Vaselli, O., Bicocchi, G., Cabassi, J., Giannini, J., Nisi, B., Chiocciora, G., 2015. A combined geochemical and isotopic study of the fluids discharged from the Montecatini thermal system (NW Tuscany, Italy). Applied Geochemistry, 59, 33-46

Cembrano, J., Lara, L., 2009. The link between volcanism and tectonics in the southern volcanic zona of the Chilean Andes: A review. Tectonophysics, 4714, 96-113.

Chandrasekharam, D., Bundschuh, J., 2008. Low-Enthalpy Geothermal Resourcesfor Power Generation. Taylor & Francis, 172p.

Clavero, J., Moreno, H., 1994. Ignimbritas Licán y Pucón: Evidencias de erupciones explosivas andesítico-basálticas postglaciales del Volcán Villarrica, Andes del Sur, 39°25'S. In Congreso Geológico Chileno, 7, 250-254.

Coleman, M., Shepherd, T., Rouse, J., Moore, G., 1982. Reduction of water with zinc forhydrogen isotope analysis. Analytical Chemistry, 54, 993-995.

D'Alessandro, W., De Gregorio, S., Dongarrà, G., Gurrieri, S., Parello, F., Parisi, B., 1997. Chemical and isotopic characterization of the gases of Mount Etna (Italy). Journal of Volcanology and Geothermal Research, 78, 65-76.

Ellis, A.J., Mahon, W.A.J., 1977. Chemistry and GeothermalSystems. Academic Press, New York.

Epstein, S., Mayeda, T., 1953. Variation of the $^{18}O/^{16}O$ ratio in natural waters. Geochimica et Cosmochimica Acta, 4, 213-224.

Favara, R., Grassa, F., Madonia, P., Valenza, M., 2001. Geochemical Processes governing changes inthe chemistry of some thermal and cold springs in Central Italy, Proc. WRI-10, Water-Rock Interaction X Int. Conference, Villasimius, Italy. Balkema Editions, 2, 811-814.

Fournier, R.O., 1977. Chemical geothermometers and mixing models for geothermal systems, Geothermics, 5, 41-50.

Fournier, R.O., 1979. A revised equation for the Na/K geothermometer. GeothermalResources Council Transactions, 5, 1-16.

Fournier, R.O., 1985. The behavior of silica in hydrothermal solutions. Reviews in Economic Geology, 2, 45-62.

Fournier, R.O., 1991. Water geothermometers applied to geothermal energy. Application of Geochemistry in Geothermal Reservoir Development. Center on Small Energy Resources, 1991, 37-69.

Fournier, R.O., Rowe, J.J., 1977. The solubility of amorphous silica in water at high temperatures and high pressures. American Mineralogist, 62, 1052-1056.

Fournier, R.O., Potter, W., 1982. A Revised and Expanded Silica (Quartz) Geothermometer. Bulletin Geothermal Resources Council (GRC), 11, 3-12.

Fournier, R.O., Marshall, W.L., 1983. Calculation of amorphous silica solubilities and cation hydration numbers in aqueous salt solutions using the concept of effective density of water. Geochimica et Cosmochimica Acta, 47, 587-596.

Giggenbach, W.F., 1988. Geothermal solute equilibria, derivation of Na-K-Mg-Cageoindicators. Geochimica et Cosmochimica Acta, 52, 2749-2765.

Giggenbach, W.F., 1992. Isotopic shift in waters from geothermal and volcanic systems along convergent plate boundaries and their origin. Earth and Planetary Science Letters, 11, 495-510.

Giggenbach, W.F., 1993. Redox control of gas compositions in Philippine volcanic–hydrothermal system. Geothermics, 22, 575-587.

Giggenbach, W.F., Goguel, R., 1989. Collection and Analysis of Geothermal and Volcanic Water and Gas Discharges. Department of Scientific and Industrial Research. Chemistry Division 4th Edition, 81 p.

Giggenbach, W.F., Poreda, R.J., 1993. Helium isotopic and chemical composition of gases from volcanic hydrothcrmal systems in the Philippines. Geothermics, 22, 369-380.

Grassa, F., Favara, R., Valenza, M., 2006. Moisture source in the Hyblean Mountains region (south-eastern Sicily, Italy): Evidence from stable isotopes signature, Applied Geochemestry, 21, 2082-2095

Hauser, A., 1997. Catastro y Caracterización de las Fuentes de Aguas Minerales y Termales de Chile. Subdirección Nacional de Geología y Minería Boletín, 50, 89p.

Hauser, A., 1989. Fuentes termales y minerales en torno a la carretera austral, Regiones X-XI, Chile: Revista Geológica de Chile**,**16, 229-239.

Held, S., Schill, E., Schneider, J., Nietschke, F., Morata, D., Neumann, T., Kohl, T., 2018. Geochemical characterization of the geothermal system at Villarrica volcano, Southern Chile; Part 1: Impacts of lithology on the geothermal reservoir. Geothermics, 74, 226–239. (Revisar nombre Nietsche)

Hervé, F., Pankhurst, R.J., Drake, R., Beek, M., Mpodozis, C., 1993. Granite generation and rapid unroofing related to strike-slip fault, Aysén, Chile. Earth and Planetary Science Letters, 120, 375-386.

Jordan, T., Burns, W., Veiga, R., Pángaro, F., Copeland, P., Kelley, Mpodozis, C., 2001. Extension and basin formation in the Southern Andes caused by increased convergencerate: A mid-Cenozoic trigger for the Andes. *Tectonics* **20**, 308-324. (Revisar nombre Kelley)

Langelier, W.F., Ludwig, H.F., 1942. Graphical method for indicating of the mineral character of natural waters. Journal of the American Water Works Association, 34**,** 335-352.

Lara, L., Moreno, H., 2004. Geología del Área Liquiñe-Neltume, Regiones de LaAraucanía y de Los Lagos. Servicio Nacional de Geología y Minería, Carta Geológica de Chile, Serie Geología Básica, 83, 23p., 1 mapa escala 1:100.000.

López-Escobar, L., Cembrano, J., Moreno, H., 1995. Geochemistry and tectonics of the Chilean Southern Andes basaltic Quaternary volcanism (37º-46ºS). Revista Geológica de Chile, 22, 219-234.

Moreno, H., Clavero, J., 2006. Geología del área del Volcán Villarrica. Servicio Nacional de Geología y Minería, Serie Geología Básica. Carta Geológica de Chile, 98, escala 1:50.000.

Moreno, H., Clavero, J., Lara, L., 1994. Actividad explosiva postglacial del Volcán Villarrica, Andes del Sur. In: Congreso Geológico Chileno, No. 7, 329-333 p. Concepción, Chile.

Moreno, R.H., 1974. Andean volcanes of Central South Chile Guide Book. Airplane Flight over active volcanoes of Central-South Chile. International Symposium on Volcanology, Santiago, Chile.

Munizaga, F., Hervé, F., Drake, R., Pankhurst, R.J., Brook, M., Snelling, N., 1988. Geochronology of the Lake Region of south-central Chile (39°-42°S): Preliminary results. Journal of South American Earth Sciences**,** 1, 309-316.

Newhall, C.G., Self, S., 1982. The volcanic explosivity index (VEI) an estimate of explosive magnitude for historical volcanism. Journal of Geophysical Research, 87(C2), 1231-1238

Pérez, Y., 1999. Fuentes de Aguas Termales de la Cordillera Andina del centro–surde Chile (39- 42° Sur). Servicio Nacional de Geología y Minería Boletín, 54, 65 p.

Petit-Breuilh, M.E., Lobato, J., 1994. Análisis comparativo de la cronología eruptiva histórica de los volcanes Llaima y Villarrica (38°-39° L.S.). In: Congreso Geológico Chileno, 7, 366-370. Concepción, Chile.

Ray, M.C., Hilton, D.R., Muñoz, J., Fischer, T.P., Shaw, A.M., 2009. The effects ofvolatile recycling, degassing and crustal contamination on the helium and carbon geochemistry of hydrothermal fluids from the Southern Volcanic Zone of Chile. Chemical Geology, 166, 38-49.

Risacher, F., Hauser, A., 2008. Catastro de las principales fuentes termales de Chile. In: Catastro Servicio Nacional de Geología y Minería, 81 p.

Risacher, F., Fritz, B., Hauser, A., 2011. Origin of components in Chilean thermal waters. Journal of South American Earth Science, 31, 153-170.

Roulleau, E., Bravo, F., Pinti, D.L., Barde-Cabusson, S., Pizarro, M., Tardani, D., Morata, D., 2017. Structural controls on fluid circulation at the Caviahue-Copahue Volcanic Complex (CCVC) geothermal area (Chile-Argentina), revealed by soil CO_2 and temperature, self-potential, and helium isotopes. Journal of Volcanology and Geothermal Research, 341, 104-118.

Rowland, J.V., Sibson, R.H., 2004. Structural controls on hydrothermal flow in a segmented rift system, Taupo Volcanic Zone, New Zealand. Geofluids, 4, 259-283.

Rowland, J.V., Simmons, S.F., 2012. Hydrologic, Magmatic, and Tectonic Controls on Hydrothermal Flow, Taupo Volcanic Zone, New Zealand: Implications for the Formation of Epithermal Vein Deposits. Economic Geology, 107, 427-457

Alfaro Sanchez, P., Reich, M., Arancibia, G., Pérez Flores, P., Cembrano, J., Driesner, T., Lizama, M., Rowland, J., Morata, D., Heinrich, C.A., Tardani, D., Campo, E., 2016. Physical, chemical and mineralogical evolution of the Tolhuaca geothermal system, southern Andes, Chile: Insights into the interplay between hydrothermal alteration and brittle deformation. Journal of Volcanology and Geothermal Research, 324, 88-104. Va al comienzo

Sepúlveda, F., Dorsch, K., Lahsen, A., Bender, S., Palacios, C., 2004. The chemical and isotopic composition of geothermal discharges from the Puyehue-Cordón Caulle area (40.5S), Southern Chile. *Geothermics*, 33, 655-673.

Sepúlveda, F., Lahsen, A., Powell, T., 2007. Gas geochemistry of the Cordón Caulle geothermal system, Southern Chile. *Geothermics*, 36, 389-420.

Sibson, R.H., 1994. Crustal stress, faulting and fluid flow. Geological Society, London, Special Publications, **78**, 69-84.

Sibson, R.H., 1996. Structural permeability of fluid-driven fault-fracture meshes. *Journal of Structural Geology,* 18, 1031-1042.

Simmons, S.F., Browne, P.R.L., 2000. Hydrothermal minerals and precious metals in the Broadlands-Ohaaki geothermal system: Implications for understanding low-sulfidation epithermal environments. Economic Geology, **95**, 971-999.

Stern, C., 2004. Active Andean volcanism: its geologic and tectonic setting. Revista Geológica de Chile, 31, 161-206.

Stern, C., Moreno, H., López-Escobar, L., Clavero, J.E., Lara, L.E., Naranjo, J.A., Parada, M.A., Skewes, M.A. 2007. Chilean Volcanoes. In: The Geology of Chile. Geological Society of Chile, 156-157.

Tardani, D., Reich, M., Roulleau, E., Takahata, N., Sano, Y., Perez-Flores, P., Sanchez Alfaro, P., Cembrano, J., Arancibia, G., 2016. Exploring the feedbacks between structure and hydrothermal fluid composition using helium, nitrogen and carbon isotopes in a long-lived intra-arc strike slip fault. Geochimica et Cosmochimica Acta, 184, 193-211.

Tassi, F., Martinez, C., Vaselli, O., Capaccioni, B., Viramonte, J., 2005. The light hydrocarbons as new geoindicators of equilibrium temperature and redox conditions of geothermal fields: evidence from El Tatio (northern Chile). Applied Geochemistry, 20, 2049-2062.

Tassi, F., Aguilera, F., Vaselli, O., Medina, E., Tedesco, D., Delgado Huertas, A., Poreda, R., Kojima, S. 2009. The magmatic and hydrothermal-dominated fumarolic system at the Active Crater of Lascar volcano, northern Chile. Bulletin of Volcanology, 71,171-183.

Thorpe, R.S., Beckinsale, R.D., Patchett, P.J., Piper, J.D.A., Davies, G.R., Evans, J.A., 1984. Journal of the Geological Society, **141**, 521-536. Falta nombre del artículo

Vaselli, O., Tassi, F., Montegrossi, G., Capaccioni, B., Giannini, L., 2006. Sampling and analysis of volcanic gases. Acta Vulcanologica, 18, 65-76.

Witter, J.B., Kress, V.C., Delmelle, P., Stix, J., 2004. Volatile degassing, petrology, and magma dynamics of the Villarrica Lava Lake, Southern Chile. Journal of Volcanology and Geothermal Research, 134, 303-337.

Legend of figures and tables

Figure1. Map of the studied región showing the principal volcanoes, hotsprings and major fault system. Modified from Held et al., 2018.

Figure 2. Map and locations of sample sites.

Figure 3. Langelier-Ludwig square diagram (Langelier and Ludwig, 1942)

Figure 4. 10He-N_2/100-Ar ternary diagram for dissolved gas samples. Compositional field for "Andesitic", "Mantle" and "Crust" (Giggenbach, 1992b) and N_2/Ar ratios of "Air" and"ASW" (air saturated water) are reported. Symbols as in Fig. 3.

Figure 5. 1000Ne-O_2/10-Ar ternary diagram for dissolved gas samples. Compositional field for "Air" and "ASW" (air saturated water) between 20-80 ºC (Tassi et al., 2005) are reported.The excess domains of the respective species are indicated. Symbols as in Fig. 3.

Figure 6. SO_4-HCO_3-Cl ternary diagram for thermal waters. Symbols as in Fig. 3.

Figure 7. δD vs. $\delta^{18}O$ binary for the thermal waters from Villarrica volcano. Symbols as in Fig. 4. Theglobal meteoric water line (GMWL; Craig 1961) is also reported.

Figure 8. Solubility of several polymorphs of silica in water. A = amorphous silica, B = opal-CT, C = α-cristobalita, D = chalcedony and E = quartz (extracted Fournier, 1991).

Figure 9. Mg^{2+}-Na^{+}-K^{+} ternary diagram (Giggenbach, 1988). The axes (Na/400-K/10-√Mg) were modified to enlarge the low temperature area of the diagram. Partial and full equilibrium curves from 40 to 220 °C are reported. Symbols as in Fig. 3.

Table 1. Chemical and stable isotopic (^{18}O-H_2O and D-H_2O, in ‰ vs. V-SMOW) composition ofthermal waters from Villarrica volcano area. Concentrations are in mg/L. Outlet temperature (°C), TDS (mg/L) and pH valuesare also reported.

Table 2.Chemical composition (in μg/L) of minor or trace elements of thermal waters from Villarrica volcano area.

Table 3.Chemical and stable isotopic (^{13}C-CO_2; in ‰ vs. V-PDB) composition of dissolved gasesfrom Villarrica volcano area. Concentrations are in mmol/mol.

Table 4. Temperatures (ºC) estimated for the fluid-mineral equilibrium, for different phases of silica.

Figure1. Map of the studied región showing the principal volcanoes, hotsprings and major fault system. Modified from Held et al., 2018.

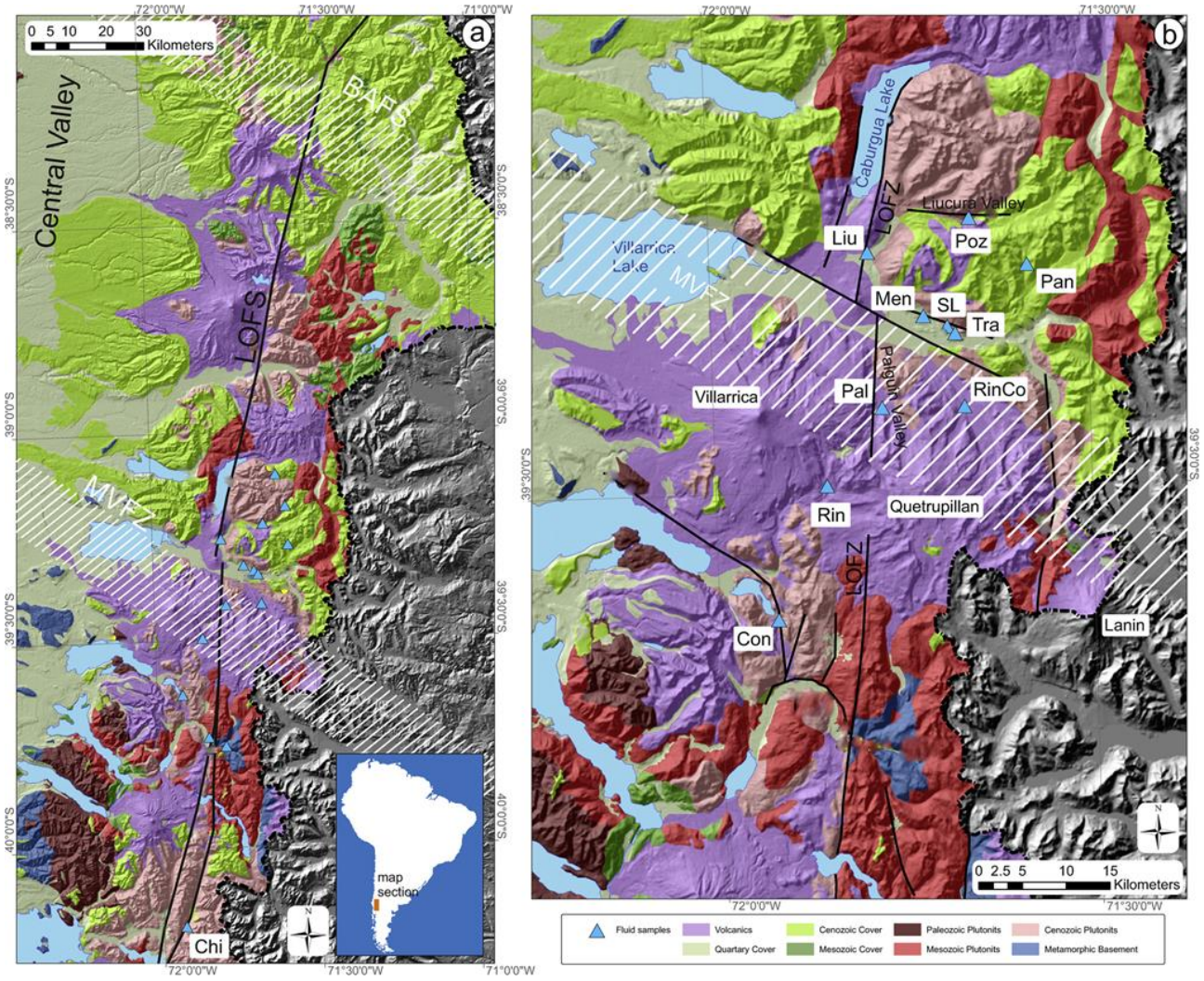

Figure 2. Map and location of sample sites.

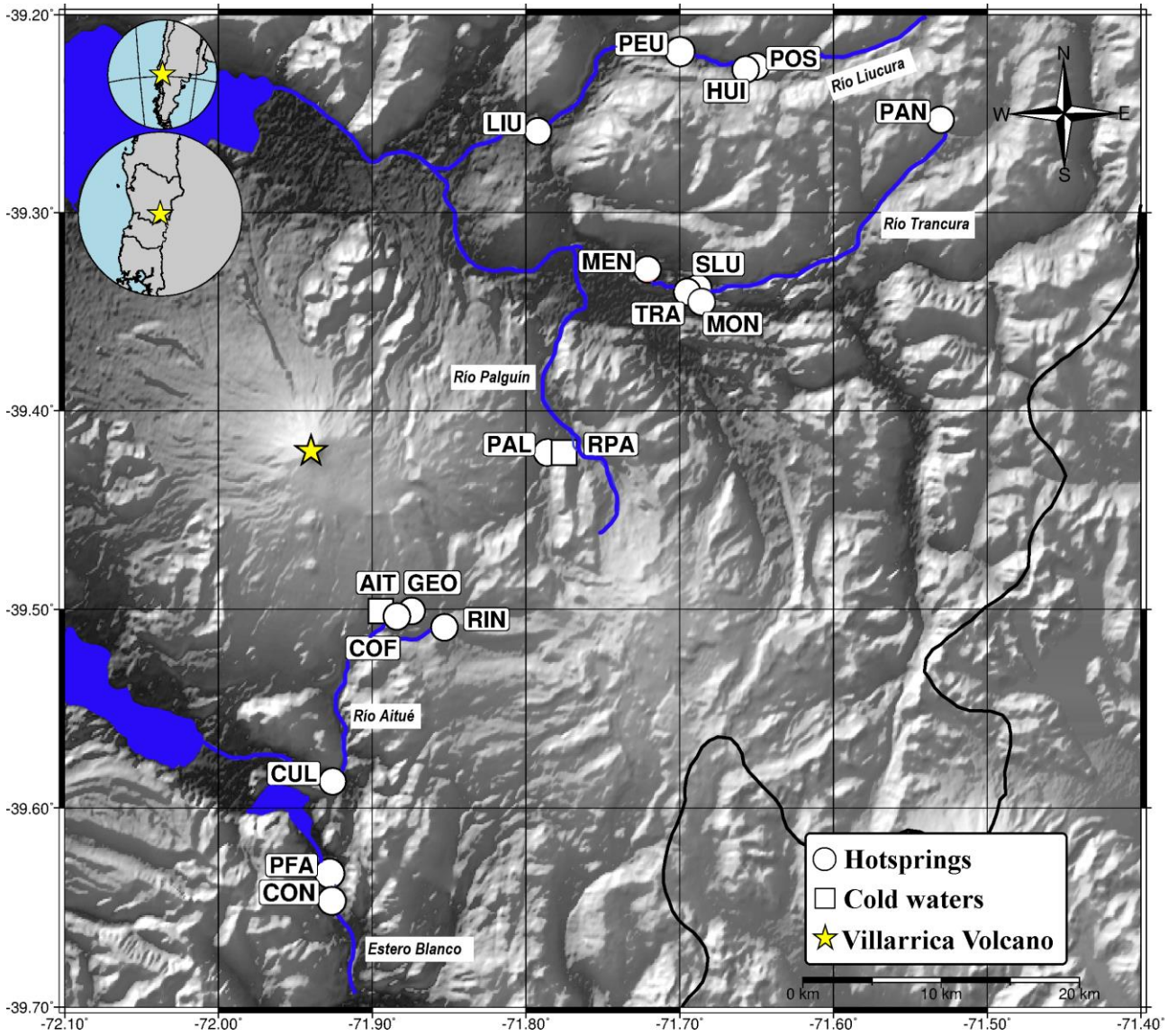

Figure 3. Langelier-Ludwig square diagram (Langelier and Ludwig, 1942)

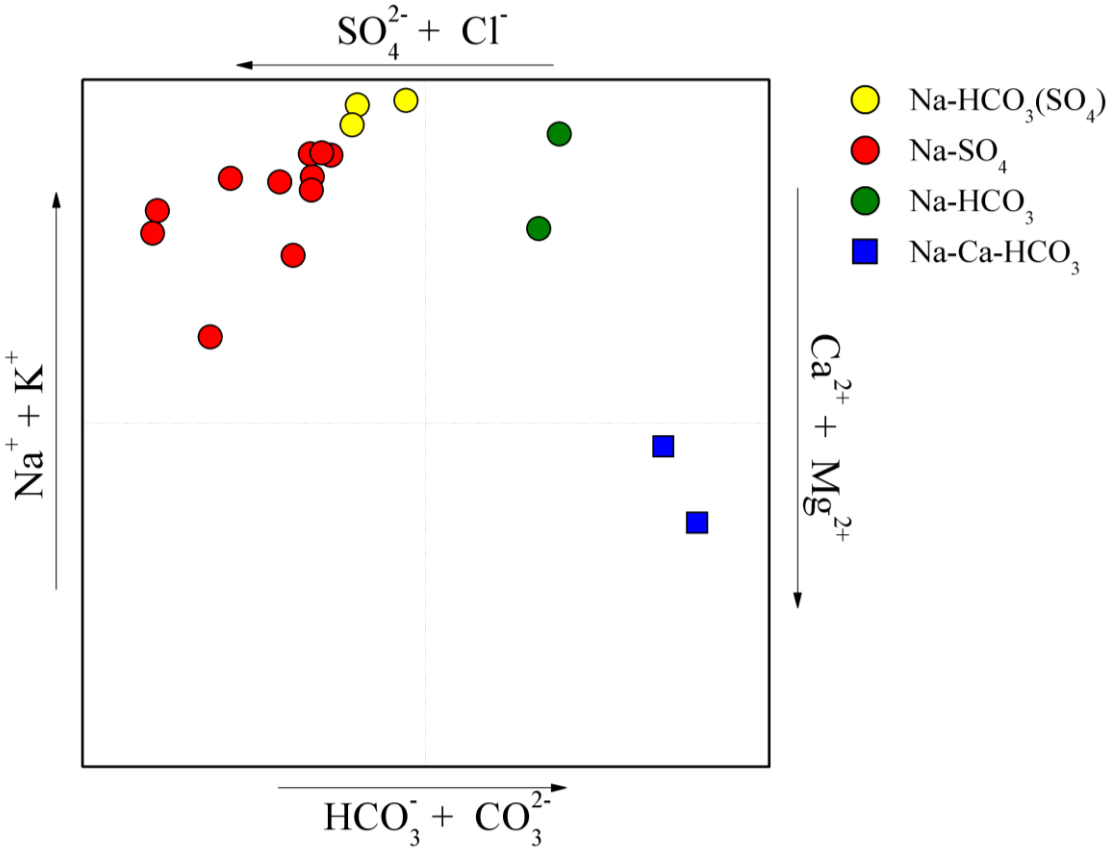

Figure 4. 10He-N_2/100-Ar ternary diagram for dissolved gas samples. Compositional field for "Andesite" and "Mantle" (Giggenbach, 1992b) and N_2/Arratios of "Air" and"ASW" (air saturated water) are reported. Symbols as in Fig. 3.

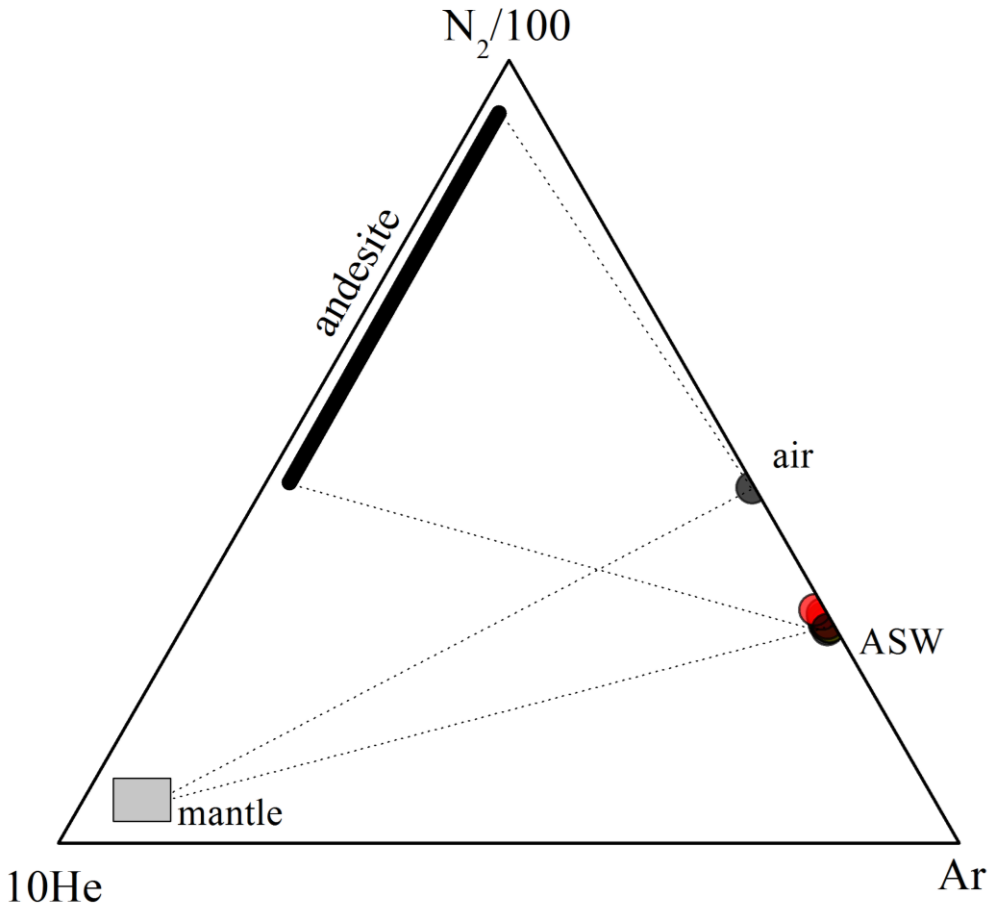

Figure 5. 1000Ne-O_2/10-Ar ternary diagram for dissolved gas samples. Compositional field for "Air" and "ASW" (air saturated water) between 20-80ºC (Tassi et al., 2005) are reported.The excess domains of the respective species are indicated. Symbols as in Fig. 3.

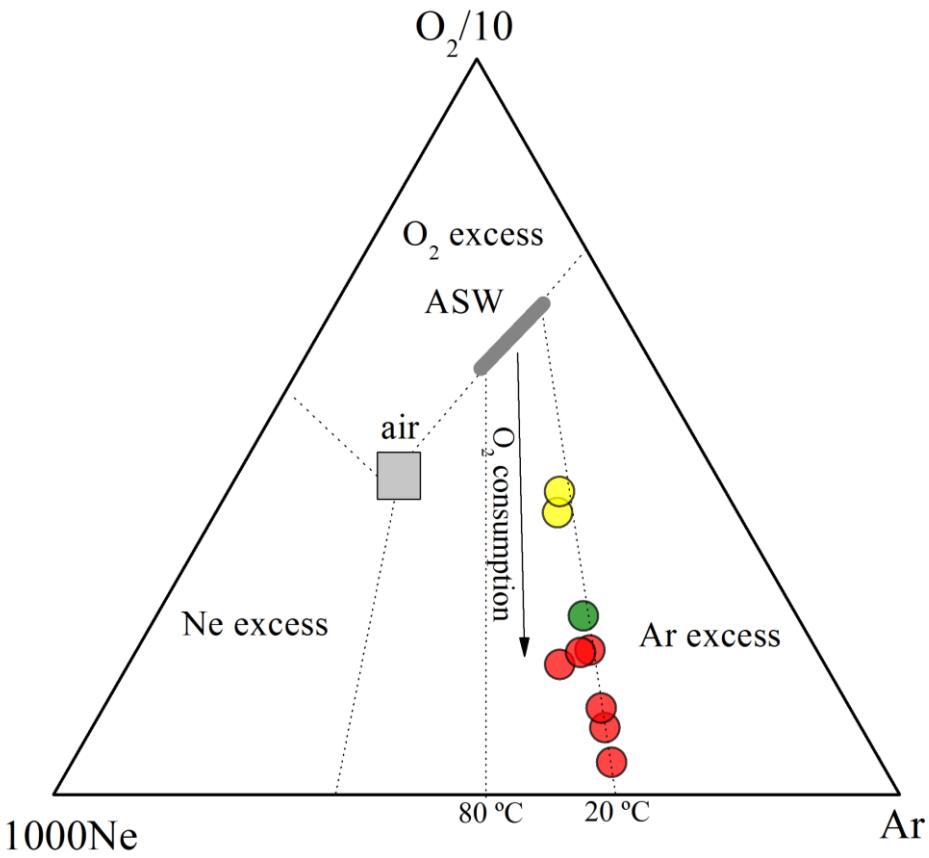

Figure 6. SO_4-HCO_3-Cl ternary diagram for thermal waters.

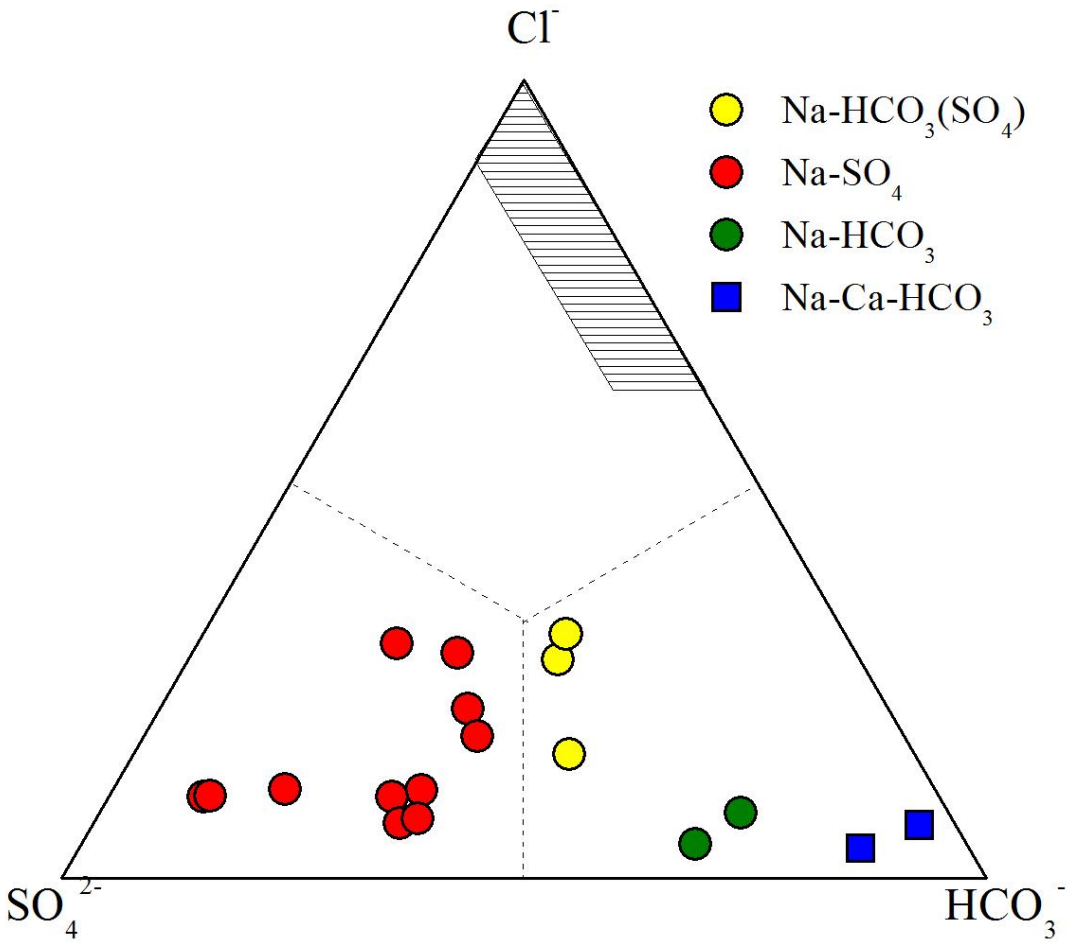

Figure 7. δD vs. $\delta^{18}O$ binary for the thermal waters from Villarrica volcano. Symbols as in Fig. 4. Theglobal meteoric water line (GMWL; Craig 1961) are also reported.

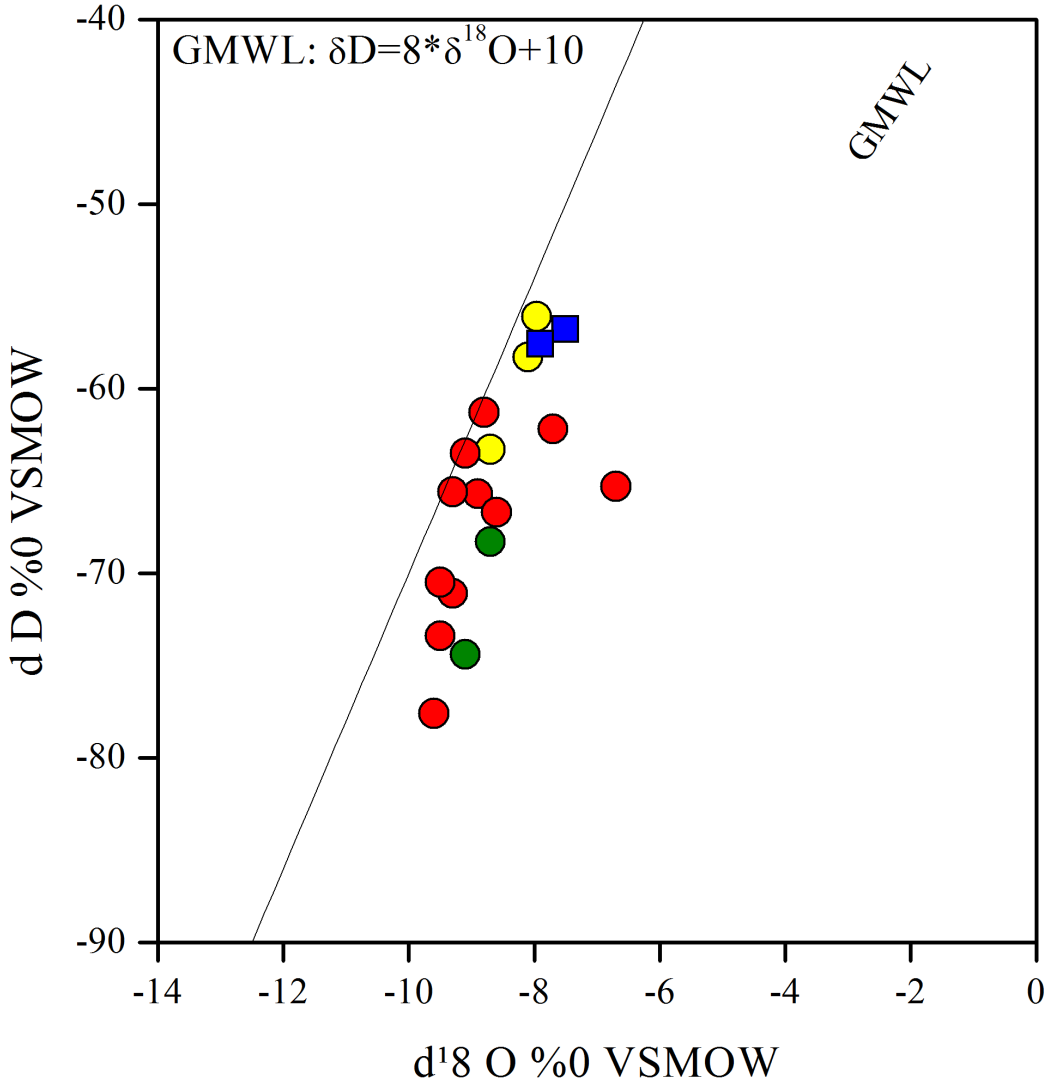

Figure 8. Solubility of several polymorphs of silica in water. A = amorphous silica, B = opal-CT, C = α-cristobalite, D = chalcedony and E = quartz (extracted from Fournier, 1991).

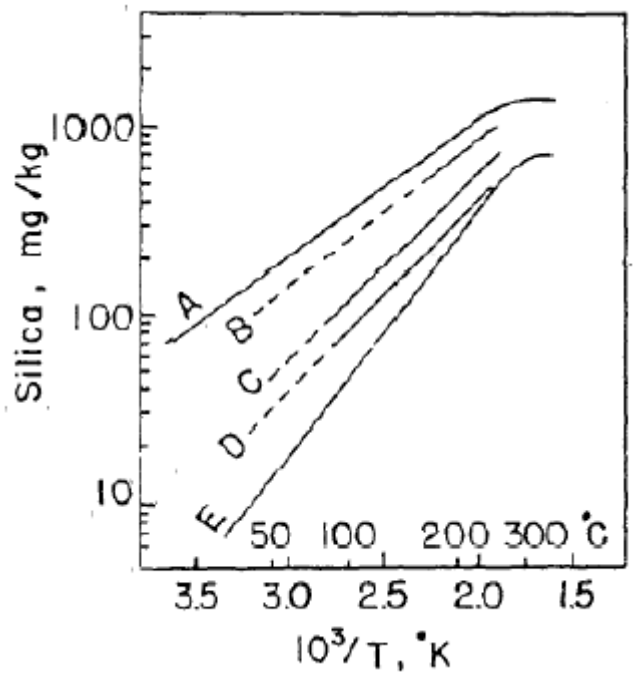

Figure 9. Mg^{2+}-Na^{+}-K^{+} ternary diagram (Giggenbach, 1988). The axes (Na/400-K/10-√Mg) weremodified to enlarge the low temperature area of the diagram. Partial and full equilibrium curves from 40 to 200 °C are reported. Symbols as in Fig. 6.

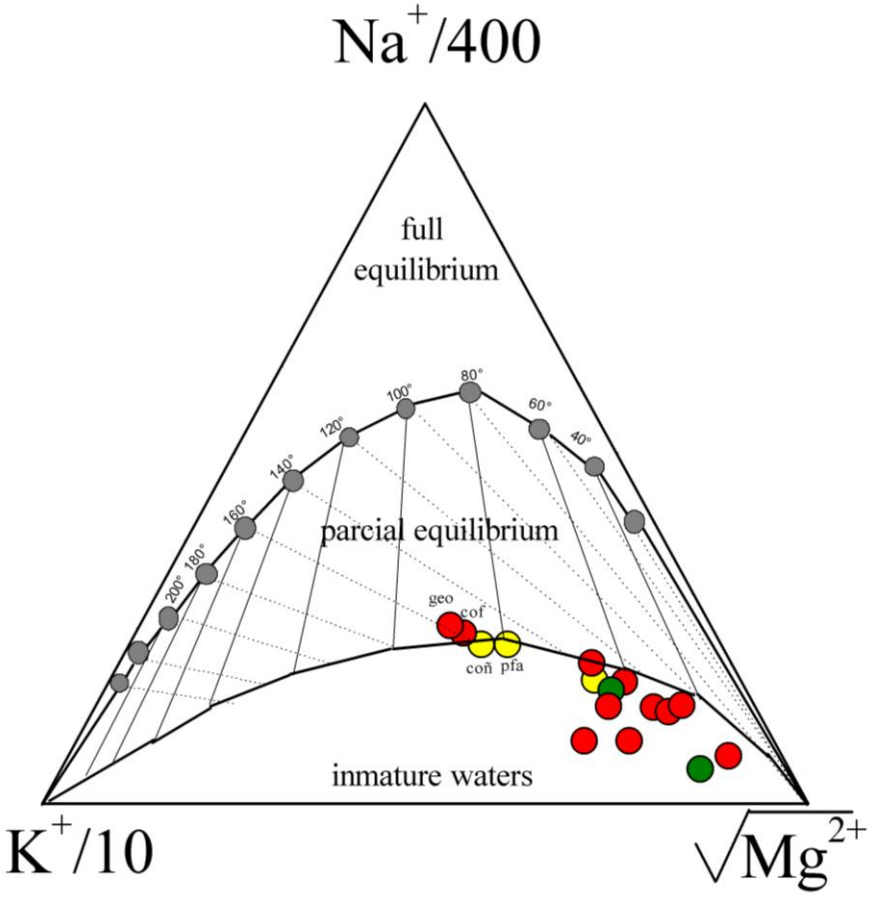

Table 1. Chemical and stable isotopic (^{18}O-H_2O and D-H_2O, in ‰ vs. V-SMOW) composition ofthermal waters from Villarrica volcano area. Concentrations are in mg/L. Outlet temperature (°C), TDS (mg/L) and pH valuesare also reported.

Location	Id	T	pH	CO_3^{-2}	HCO_3^-	F^-	Ca^{+2}	Mg^{+2}	Na^+	K^+	Li^+	SO_4^{-2}	Cl^-	B	SiO_2	TDS	δ D ‰	δ^{18} O ‰
Coñaripe	CON	71	8,3	0	123	1,2	5,0	0,5	140	4,8	0,1	100	84	3,2	7,5	418	-58	-8,1
Culán	CUL	48	8,7	0	82	0,8	2	0,4	75	2,2	0,04	65	27	0,5	15	227	-63	-8,7
El Rincon	RIN	33	8,4	0	65	0,8	11	1,8	73	5,0	0,06	108	21	0,8	19	267	-66	-8,9
Geometricas	GEO	66	8,0	0	44	1,0	47	0,5	160	5,4	0,1	342	44	2,2	60	656	-65	-6,7
Huife	HUI	52	7,9	8,1	36	1,1	12	0,5	73	1,6	0,06	82	49	0,5	9	258	-71	-9,3
Liucura	LIU	30	8,6	0	63	0,7	12	1,9	69	3,6	0,02	86	40	0,5	41	258	-73	-9,5
Posones	POS	42	7,2	0	52	1,1	12	0,9	72	1,7	0,06	78	51	0,6	11	256	-71	-9,5
Menetue	MEN	40	8,5	0	69	2,4	20	5,0	71	1,8	0,08	133	23	0,2	90	308	-61	-8,8
Montevivo	MON	43	7,1	0	68	0,4	7,0	1,5	29	1,7	0,02	30	4,4	0,1	28	114	-68	-8,7
Palguín	PAL	42	8,6	0	102	1,2	3,3	1,3	51	2,6	0,02	33	12	0,3	51	163	-74	-9,1
Panqui	PAN	52	8,3	0	45	0,2	39	0,6	64	2,2	0,06	170	27	0,4	47	343	-78	-9,6
Pellaifa	PFA	62	7,8	0	72	0,9	5,5	0,3	80	2,4	0,14	55	56	1,8	47	249	-56	-8,0
Peumayen	PEU	35	9,2	0	51	1,6	7,1	0,2	58	1,3	0,02	65	25	0,1	32	194	-67	-8,6
San Luis	SLU	35	9,3	15	36	1,3	6,1	0,6	54	1,2	0,02	65	7,4	0,1	60	178	-64	-9,1
Trancura	TRA	37	8,9	15	35	1,3	5,8	0,5	52	0,9	0,02	58	7,5	0,1	43	168	-66	-9,3
Cofre	COF	33	9,0	12	37	0,8	33	0,3	137	4,6	0,2	267	35	2,4	n.d	537	-62	-7,7
Rio Aitue	AIT	4	7,5	0	23	0,09	5,0	0,3	2,3	0,6	0,02	1,0	1,7	0,2	n.d	23	-58	-7,9
Rio Palguín	RPA	7	7,3	0	34	0,07	5,2	1,9	5,0	1,2	0,02	4,7	1,5	0,1	17	38	-57	-7,5

Table 2. Chemical composition (in mg/L) of minor or trace elements of thermal waters from Villarrica volcano area.

Location	Id	Al	Sb	As	Ba	Be	B	Cd	Co	Cu	Cr	Sn	P	Fe	Mn	Mo	Ag	Pb	Se	Va	Zn
Coñaripe	CON	0,08	0,01	1,185	0,01	0,002	3,2	0,002	0,002	0,01	0,002	0,003	0,05	0,01	0,01	0,02	0,002	0,002	0,01	0,004	0,01
Culán	CUL	0,1	0,01	0,061	0,01	0,002	0,52	0,002	0,002	0,01	0,001	0,003	0,05	0,01	0,003	0,02	0,002	0,002	0,01	0,004	0,01
El Rincon	RIN	0,02	0,01	0,05	0,01	0,002	0,793	0,002	0,002	0,01	0,001	0,003	0,05	0,01	0,003	0,01	0,002	0,002	0,01	0,02	0,01
Geometricas	GEO	0,02	0,01	0,166	0,01	0,002	2,183	0,002	0,002	0,01	0,001	0,003	0,05	0,01	0,003	0,01	0,002	0,002	0,01	0,003	0,01
Huife	HUI	0,02	0,01	0,082	0,01	0,002	0,538	0,002	0,002	0,01	0,002	0,003	0,05	0,01	0,003	0,02	0,002	0,002	0,01	0,003	0,01
Liucura	LIU	0,02	0,01	0,03	0,01	0,002	0,475	0,002	0,002	0,01	0,003	0,003	0,05	0,01	0,003	0,01	0,002	0,002	0,01	0,02	0,01
Posones	POS	0,02	0,01	0,084	0,01	0,002	0,615	0,002	0,002	0,01	0,001	0,003	0,05	0,01	0,003	0,01	0,002	0,002	0,01	0,003	0,01
Menetue	MEN	0,3	0,01	0,02	0,01	0,002	0,245	0,002	0,002	0,01	0,001	0,003	0,05	0,03	0,3	0,02	0,002	0,002	0,01	0,003	0,01
Montevivo	MON	0,02	0,01	0,01	0,01	0,002	0,1	0,002	0,002	0,01	0,001	0,003	0,05	0,01	0,003	0,01	0,002	0,002	0,01	0,004	0,01
Palguín	PAL	0,03	0,01	0,063	0,01	0,002	0,3	0,002	0,002	0,01	0,001	0,003	0,05	0,01	0,003	0,01	0,002	0,002	0,01	0,01	0,01
Panqui	PAN	0,02	0,01	0,05	0,01	0,002	0,447	0,002	0,002	0,01	0,002	0,003	0,05	0,01	0,003	0,01	0,002	0,002	0,01	0,003	0,01
Pellaifa	PFA	0,02	0,01	1,0	0,01	0,002	1,83	0,002	0,002	0,01	0,001	0,003	0,05	0,03	0,003	0,02	0,002	0,002	0,01	0,003	0,01
Peumayen	PEU	0,02	0,01	0,02	0,01	0,002	0,132	0,002	0,002	0,01	0,001	0,003	0,05	0,01	0,003	0,03	0,002	0,002	0,01	0,003	0,01
San Luis	SLU	0,02	0,01	0,01	0,01	0,002	0,08	0,002	0,002	0,01	0,001	0,003	0,05	0,01	0,003	0,02	0,002	0,002	0,01	0,004	0,01
Trancura	TRA	0,02	0,01	0,02	0,01	0,002	0,07	0,002	0,002	0,01	0,001	0,003	0,05	0,04	0,003	0,02	0,002	0,002	0,01	0,003	0,01
Cofre	COF	0,02	0,01	0,1	0,01	0,002	2,4	0,002	0,002	0,01	0,001	0,003	0,05	0,01	0,003	0,01	0,002	0,002	0,01	0,005	0,01
Rio Aitue	AIT	0,02	0,01	0,01	0,05	0,002	0,2	0,002	0,002	0,01	0,001	0,003	0,05	0,01	0,003	0,01	0,002	0,002	0,01	0,008	0,01
Rio Palguín	RPA	0,02	0,01	0,01	0,01	0,002	0,1	0,002	0,002	0,01	0,001	0,003	0,05	0,01	0,003	0,01	0,002	0,002	0,01	0,007	0,01

Table 3. Chemical and stable isotopic (^{13}C-CO_2; in ‰ vs. V-PDB) composition of dissolved gasesfrom Villarrica volcano area. Concentrations are in mmol/mol.

Location	Id	CO_2	N_2	CH_4	Ar	O_2	Ne	He	$\delta\,^{13}C$-CO_2
Culán	CUL	139	677	0,03	18	167	0,009	0,02	-25,2
El Rincon	RIN	259	665	0,03	17	59	0,01	0,02	-22,3
Geometricas	GEO	378	585	0,07	15	22	0,007	0,02	-22,4
Menetue	MEN	90	814	0,03	20	75	0,01	0,02	-16,9
Palguín	PAL	220	682	0,02	17	81	0,008	0,02	-13,9
Pellaifa	PFA	74	713	0,01	19	194	0,009	0,01	-17,6
San Luis	SLU	283	641	0,02	16	60	0,009	0,01	-18,8
Trancura	TRA	157	786	0,02	19	38	0,009	0,02	-21,8
Cofre	COF	163	805	0,08	19	13	0,009	0,03	-23,9

Table 4. Temperatures (ºC) estimated for the fluid-mineral equilibrium, for different phases of silica.

Location	Id	Quartz without loss of steam	Quartz with maximum steam loss	Chalcedony	α-cristobalite	Amorphous silica
Coñaripe	CON	30	39	-3	-17	-73
Culán	CUL	53	60	21	4	-55
El Rincon	RIN	62	67	29	12	-48
Geometricas	GEO	110	110	81	60	-7
Huife	HUI	36	44	3	-12	-68
Liucura	LIU	92	94	62	42	-22
Posones	POS	42	50	10	-6	-63
Menetue	MEN	131	128	104	81	12
Montevivo	MON	76	80	45	27	-35
Palguín	PAL	103	103	73	52	-13
Panqui	PAN	99	100	69	49	-16
Pellaifa	PFA	99	100	69	49	-16
Peumayen	PEU	82	86	51	32	-31
San Luis	SLU	58	64	25	9	-51
Trancura	TRA	110	110	81	60	-7
Cofre	COF	95	96	64	44	-20